Presented at the 9th Atmospheric Radiation Measurement Program Science Team Meeting, 22-26 March, 1999, San Antonio, TX.

Observations of Integrated Water Vapor and Cloud Liquid Water at SHEBA

James Liljegren

Ames Laboratory
Ames, IA
515.294.8428
liljegren@ameslab.gov

Introduction

In the Arctic water vapor and clouds influence the surface radiation balance to a greater extent than at lower latitudes. Because the integrated water vapor is often less than 5 mm, substantial radiative cooling occurs in the 20 μm infrared region whereas this region is normally opaque at lower latitudes having greater water vapor amounts. Thin liquid water clouds also significantly affect the surface radiation balance.

Integrated water vapor and cloud liquid water at the SHEBA (Surface Heat Budget of the Arctic) ice station were measured continuously over a 12-month period with a microwave radiometer (MWR; see Figure 1) that was among the suite of instruments deployed at SHEBA by the Atmospheric Radiation Measurement (ARM) Program.

Calibration

Beginning in December 1997 the radiometer was operated in a continuous elevation angle-scanning mode in order to permit calibration updates whenever the sky was clear. The algorithms applied *a posteriori* to the SHEBA microwave radiometer data to derive a continuous calibration from the angular scans were essentially identical to those developed for continuous real-time calibration of the other ARM microwave radiometers. (See the companion paper by Liljegren for details of the calibration algorithms.)

General Results

Figure 2 presents the record of integrated water vapor (IWV), integrated liquid water (ILW) and surface air temperature at the SHEBA ice station for the period from December 1997 through September 1998. The wide range of IWV, from 0.1 to over 2.0 cm, is evident. Note also the marked changes that occur once the temperature reaches 0 °C.

Below freezing the IWV and ILW are generally small and variations in IWV correlate well with variations in the surface air temperature as warmer (and more moist) air masses move through the region. However, once the surface air temperature reaches 0 °C, the net radiation no longer goes to heating the air but rather to melting snow and

evaporating water. Once this happens and melt ponds develop, the IWV (and ILW) dramatically increase and are no longer well correlated with the surface air temperature.

Water Vapor Comparisons

Radiosondes were launched twice per day, except during the FIRE IFO when they were launched four times per day. These provide an opportunity for comparing IWV with the microwave radiometer. The comparison of IWV derived from radiosondes with that from the microwave radiometer is presented in Figure 3 for clear sky conditions.

The agreement between the MWR and the radiosondes is very good down to 1 mm! (The calibration correction recently developed by Vaisala for the sonde relative humidity sensor was not applied. For such low water vapor amounts the correction would not be significant. See the accompanying papers by Liljegren and Lesht for more about the effect of this correction at the SGP.)

In Figure 4 radiometric brightness temperatures measured with the MWR are compared with calculations based on the Liebe 87 absorption model in order to examine the model performance in the limit of low water vapor where the microwave signal is dominated by oxygen emission. The similar values for the slope indicate that the water vapor absorption model appears correct. The 0.7 K difference in the intercepts suggests the oxygen absorption model may be too low.

Liquid Water Comparisons

During the FIRE IFO periods the SHEBA ice camp was over flown by several research aircraft, including the NCAR C-130 which was equipped with a Gerber PVM liquid water content probe. As shown in Figures 5a and 5b, comparison of the integrated liquid water from the MWR with ILW from the Gerber PVM probe generally exhibit good agreement, although it appears that on May 15 the cloud sampled by the aircraft did not always pass over the radiometer.

Continuously scanning the sky between ±45° of zenith at 5° intervals permitted the time-varying spatial structure of cloud liquid water to be observed. Figures 6 and 7 represent the integrated liquid water distribution from +45° to -45° about zenith. The values have been adjusted to zenith (measured opacities were divided by the sine of the elevation angle prior to applying the retrieval.) These figures reveal significant spatial variations in the ILW that contribute to spatial variations in the solar and thermal radiation fields that would not be observed by either zenith-only or hemispherically-integrating sensors.

Conclusions

The ARM microwave radiometer provided a continuous record of integrated water vapor and liquid water at the SHEBA ice station. The water vapor measurements

(down to 1 mm) exhibited very good agreement with radiosondes. Measured brightness temperatures were in agreement with the Liebe 87 water vapor absorption model. Integrated liquid water measurements generally agreed very well with the Gerber PVM on the NCAR C-130 aircraft.

Figures

Figure 1. The ARM microwave radiometer deployed at SHEBA.

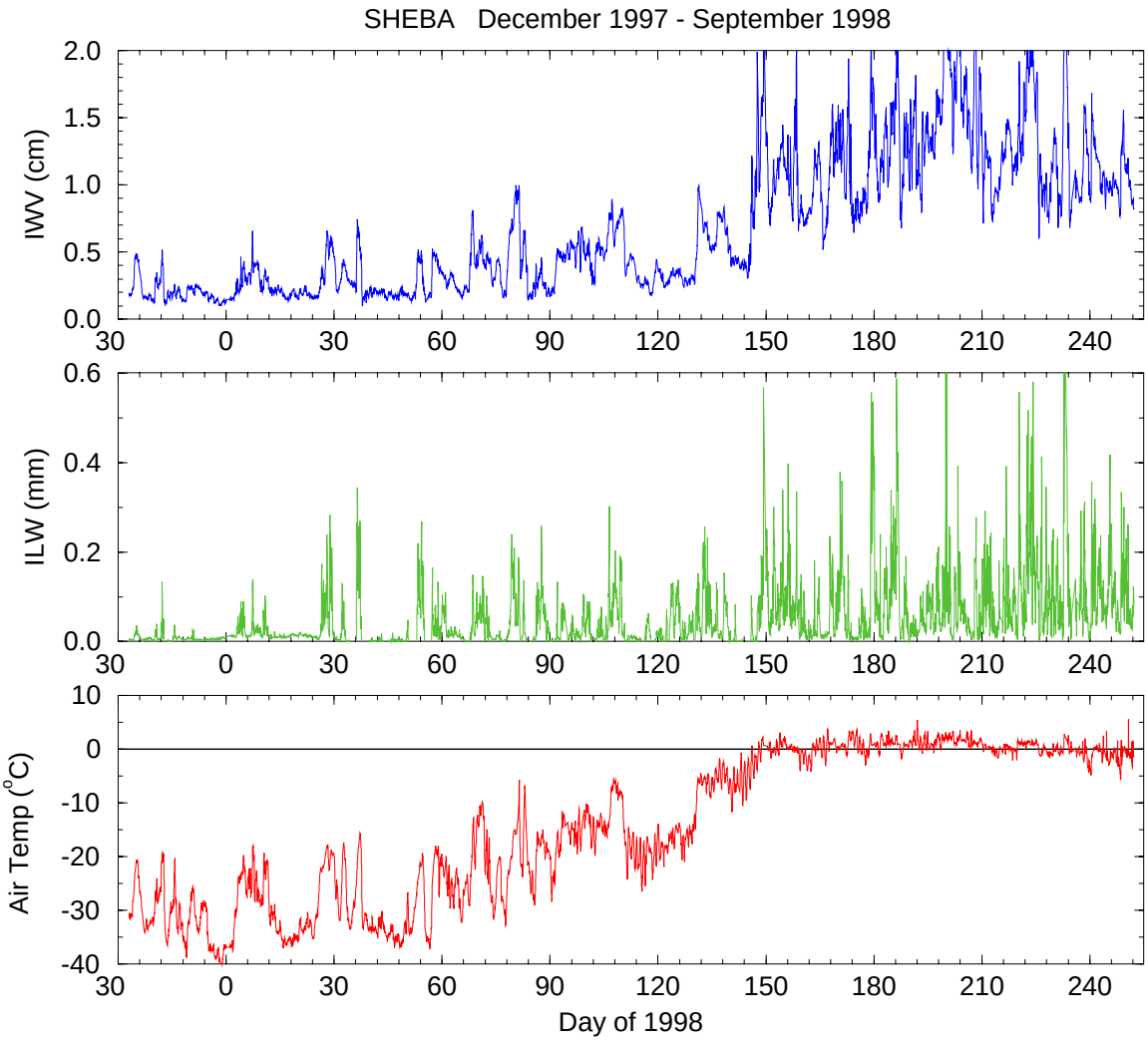

Figure 2. The hourly record of integrated water vapor (IWV), integrated liquid water (ILW) and surface air temperature at the SHEBA ice station.

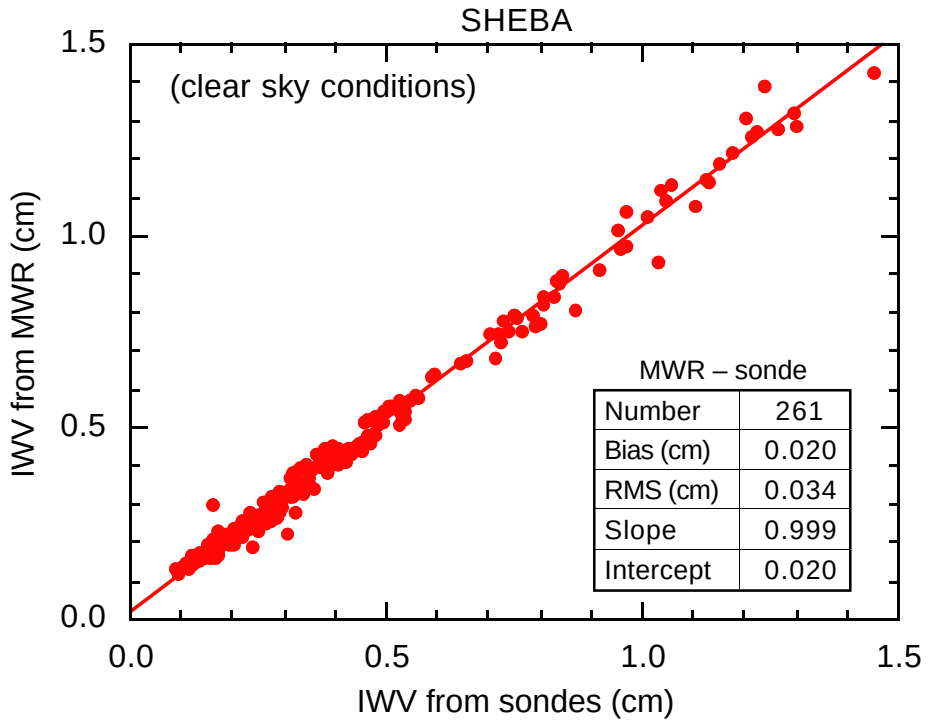

Figure 3. Comparison of integrated water vapor derived from radiosondes and the microwave radiometer.

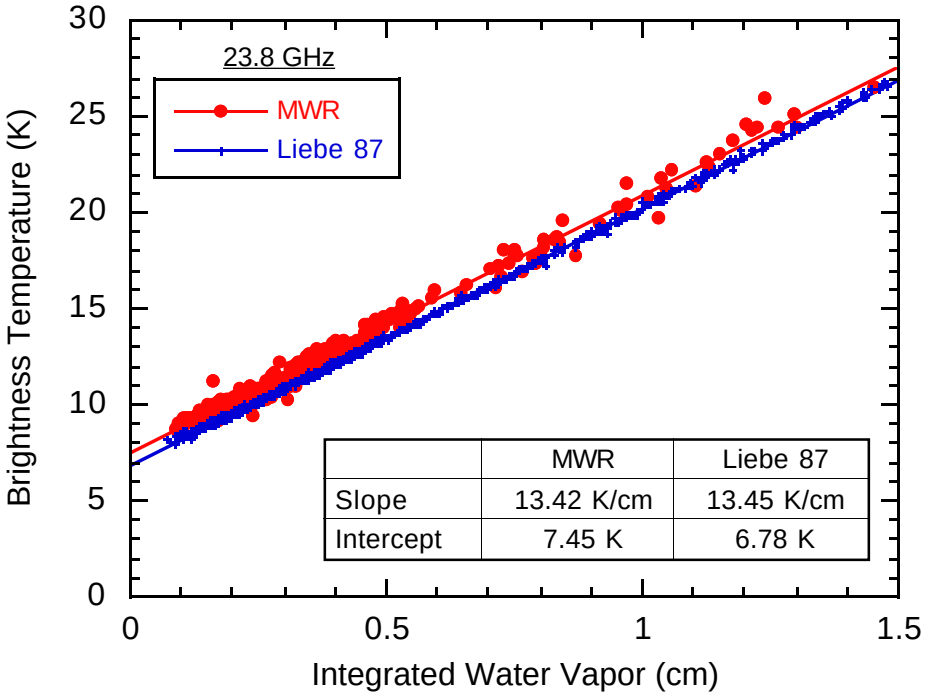

Figure 4. Comparison of brightness temperatures measured with the microwave radiometer and calculated using the Liebe 87 model. The integrated water vapor along the abscissa is derived from the radiosondes.

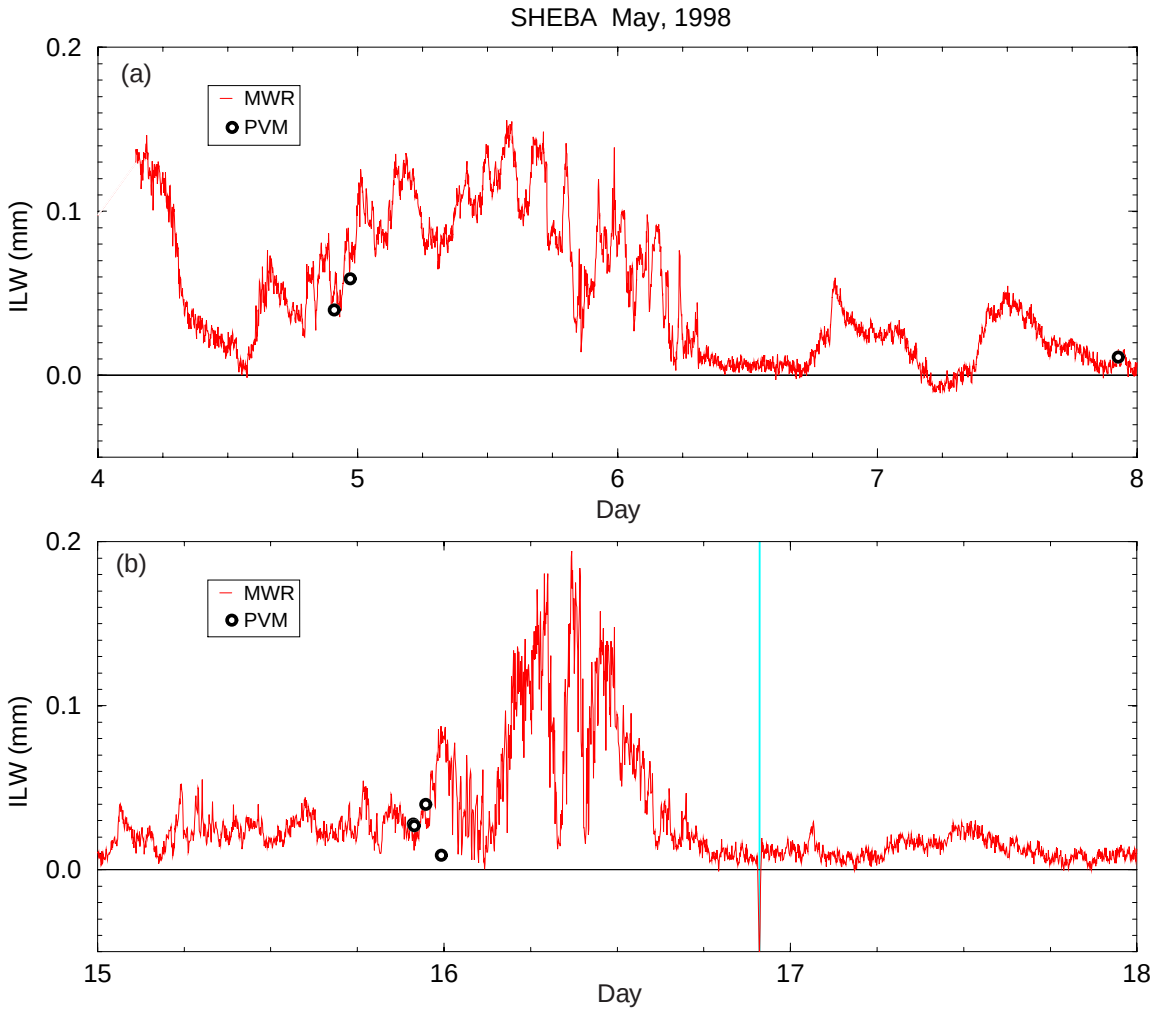

Figure 5. Integrated liquid water from the MWR and Gerber PVM. (a) 4-7 May; (b) 15-17 May. The light blue vertical bar in (b) indicates an anomaly in the ILW from the MWR detected by the quality control processing.

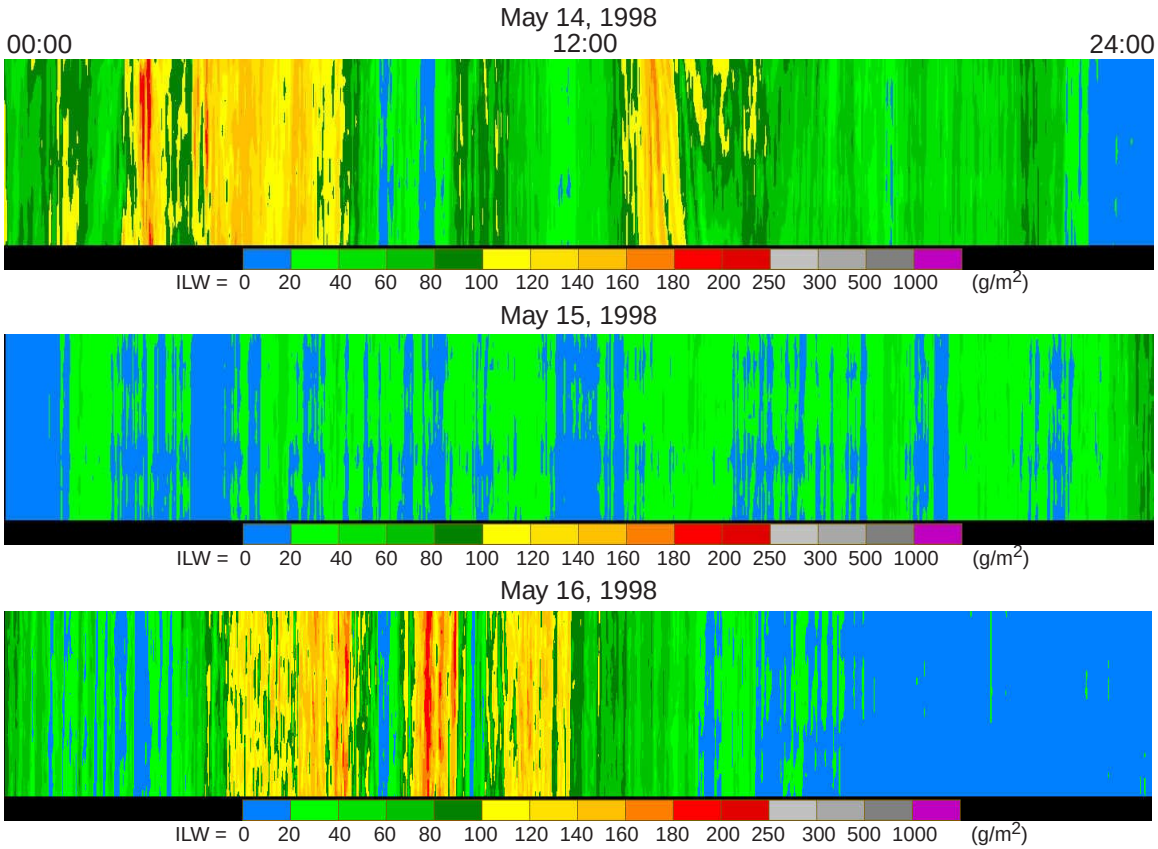

Figure 6. Spatial distribution of ILW (adjusted to zenith) for 14-17 May, 1998. (1000 g/m^2 = 1 mm) The top of each plot is +45° from zenith; the bottom is -45° from zenith.

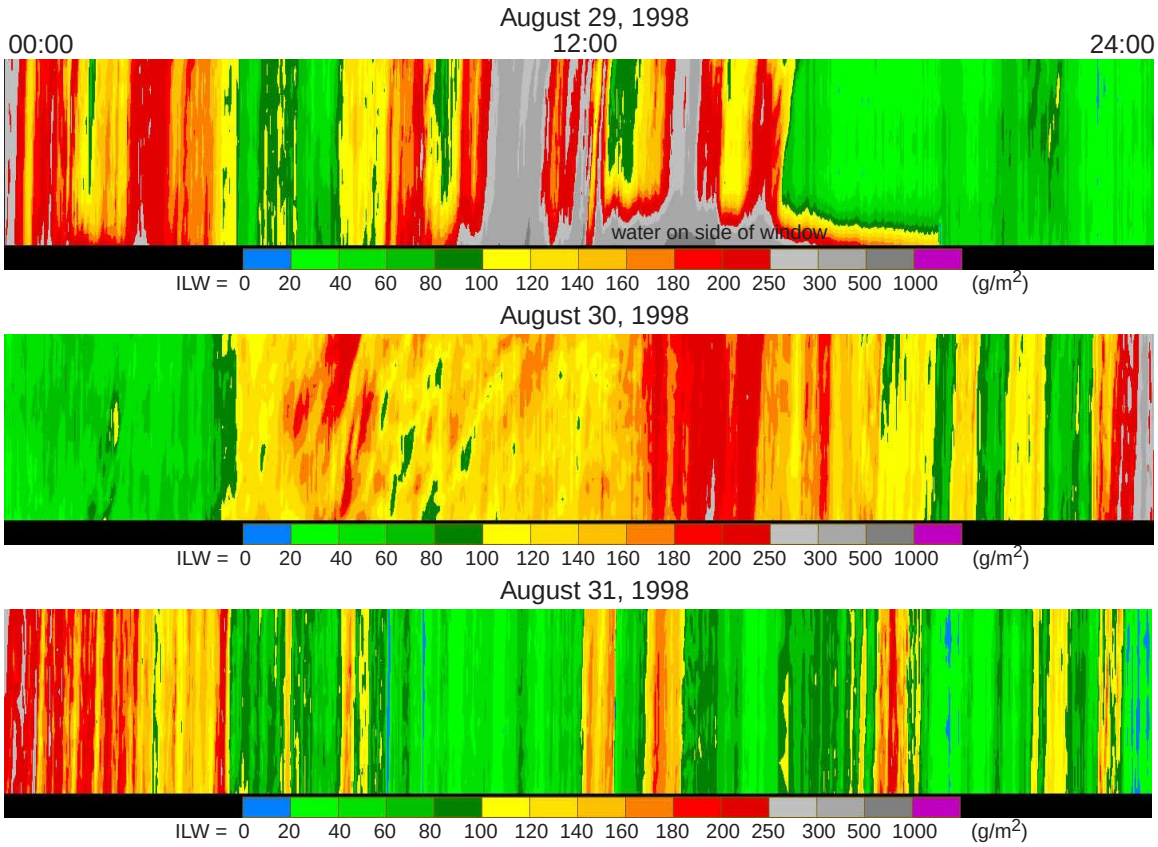

Figure 7. Spatial distribution of ILW (adjusted to zenith) for 29-31 August, 1998. (1000 g/m^2 = 1 mm) The occurrence of water on the radiometer window is evident on August 29.